NONLINEAR VIBRATIONS AND ENERGY DISTRIBUTION OF CARBON NANOTUBES

Angelo Oreste Andrisano
Department of Engineering "Enzo Ferrari", University of Modena and Reggio Emilia, Italy
E-mail: angelooreste.andrisano@unimore.it

Leonid I. Manevitch
N.N. Semenov Institute of Chemical Physics, Russian Academy of Sciences, Moscow, Russia
E-mail: lmanev@chph.ras.ru

Francesco Pellicano
Department of Engineering "Enzo Ferrari", University of Modena and Reggio Emilia, Italy
E-mail: francesco.pellicano@unimore.it

Matteo Strozzi
Department of Engineering "Enzo Ferrari", University of Modena and Reggio Emilia, Italy
E-mail: matteo.strozzi@unimore.it

Abstract. *The nonlinear vibrations of Single-Walled Carbon Nanotubes are analysed. The Sanders-Koiter thin shell theory is applied in order to obtain the elastic strain and kinetic energy. The carbon nanotube deformation is described in terms of axial, circumferential and radial displacement fields. The theory considers geometric nonlinearities due to large amplitude of vibration. The displacement fields are expanded by means of a double series based on harmonic functions for the circumferential variable and Chebyshev polynomials for the longitudinal variable. The Rayleigh-Ritz method is applied to obtain approximate natural frequencies and mode shapes. Free boundary conditions are considered. In the nonlinear analysis, the three displacement fields are re-expanded by using approximate eigenfunctions. An energy approach based on the Lagrange equations is then considered to obtain a set of nonlinear ordinary differential equations. The total energy distribution of the shell is studied by considering combinations of different vibration modes. The effect of the conjugate modes is analysed.*

Keywords*: nonlinear vibrations, energy distribution, carbon nanotubes*

1. INTRODUCTION

Carbon Nanotubes were discovered in 1991 by Iijima [1], who first analysed the synthesis of molecular carbon structures in the form of fullerenes and reported the preparation of the carbon nanotubes, as helical microtubules of graphitic carbon.

Rao et al. [2] studied the vibrations of SWNTs by Raman scattering experimental techniques with laser excitation wavelengths in the range of the nanometres. They observed Raman peaks, which correspond to vibrational modes of the nanotubes.

Gupta et al. [3] simulated the mechanical behaviour of SWNTs with free edges by using the MD potential. They considered the effect of the chirality and geometry on the natural frequencies of longitudinal, torsional and inextensional modes.

Arghavan and Singh [4] carried out a numerical study on the free and forced vibrations of SWNTs considering the FE method. They studied different boundary conditions, obtaining natural frequencies, mode shapes, time histories and spectra.

Wang et al. [5] examined applicability and limitations of different simplified models of elastic cylindrical shells for general cases of static buckling and free vibrations. They considered Flugge, Donnell thin shell and Donnell shallow shell models.

Strozzi et al. [6] considered the linear vibrations of SWNTs for different boundary conditions in the framework of the Sanders-Koiter thin shell theory. They studied several types of nanotubes by varying aspect ratio and chirality in a wide range of the natural frequency spectrum.

In the present paper, the nonlinear vibrations of SWNTs are analysed. The Sanders-Koiter thin shell theory is applied. The displacement fields are expanded by means of a double series based on harmonic functions for the circumferential variable and Chebyshev polynomials for the longitudinal variable.

The Rayleigh-Ritz method is applied to obtain approximate natural frequencies and mode shapes. Free boundary conditions are considered.

In the nonlinear analysis, the three displacement fields are re-expanded by using approximate eigenfunctions.

The Lagrange equations are considered in order to obtain a set of nonlinear ordinary differential equations.

The total energy distribution is studied by considering different combined modes. The effect of the conjugate modes participation on the energy distribution is analysed.

2. SANDERS-KOITER THEORY

In Figure 1, a circular cylindrical shell having radius R, length L and thickness h is shown; a cylindrical coordinate system (O; x, θ, z) is considered to take advantage from the axial symmetry of the structure, the origin O of the reference system is located at the centre of one end of the cylindrical shell.

Three displacement fields are represented: longitudinal u (x, θ, t), circumferential v (x, θ, t) and radial w (x, θ, t), where the radial displacement field w is considered positive outward, (x, θ) are the longitudinal and angular coordinates of an arbitrary point on the middle surface, z is the radial coordinate along the thickness h and t denotes the time variable.

Parameter ($\eta = x/L$) is the nondimensional longitudinal coordinate of the shell, ($\beta = h/L$) denotes a nondimensional parameter and τ is the nondimensional time variable, which is obtained by introducing a reference natural frequency ω_0.

3. ELASTIC STRAIN ENERGY

The nondimensional elastic strain energy of a cylindrical shell, by neglecting the transverse normal stress σ_z (plane stress) and shear strains (γ_{xz}, $\gamma_{\theta z}$) (Kirchhoff's hypothesis), is written in the form

$$\tilde{U} = \frac{1}{2}\int_0^1\int_0^{2\pi}\left(\tilde{\varepsilon}_{x,0}^2 + \tilde{\varepsilon}_{\theta,0}^2 + 2\nu\tilde{\varepsilon}_{x,0}\tilde{\varepsilon}_{\theta,0} + \frac{(1-\nu)}{2}\tilde{\gamma}_{x\theta,0}^2\right)d\eta d\theta + \frac{1}{2}\frac{\beta^2}{12}\int_0^1\int_0^{2\pi}\left(\tilde{k}_x^2 + \tilde{k}_\theta^2 + 2\nu\tilde{k}_x\tilde{k}_\theta + \frac{(1-\nu)}{2}\tilde{k}_{x\theta}^2\right)d\eta d\theta \tag{1}$$

where ($\tilde{\varepsilon}_{x,0}$, $\tilde{\varepsilon}_{\theta,0}$, $\tilde{\gamma}_{x\theta,0}$) denote the nondimensional middle surface strains and ($\tilde{k}_x$, $\tilde{k}_\theta$, $\tilde{k}_{x\theta}$) denote the nondimensional middle surface changes in curvature and torsion.

4. KINETIC ENERGY

The nondimensional kinetic energy of a cylindrical shell is given by

$$\tilde{T} = \frac{1}{2}\int_0^1\int_0^{2\pi}(\tilde{u}'^2 + \tilde{v}'^2 + \tilde{w}'^2)d\theta d\eta = \frac{1}{2}\int_0^1\int_0^{2\pi}\left[\left(\frac{d\tilde{u}}{d\tau}\right)^2 + \left(\frac{d\tilde{v}}{d\tau}\right)^2 + \left(\frac{d\tilde{w}}{d\tau}\right)^2\right]d\theta d\eta \tag{2}$$

where ($\tilde{u},\tilde{v},\tilde{w}$) denote the nondimensional displacement fields and ($\tilde{u}',\tilde{v}',\tilde{w}'$) denote the nondimensional velocity fields.

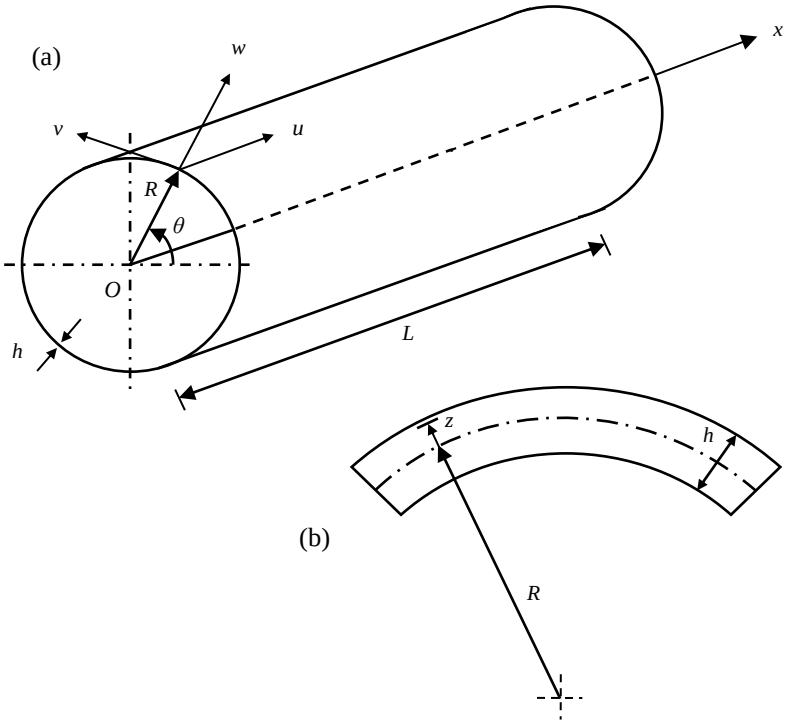

Figure 1. Geometry of the shell. (a) Complete shell; (b) cross-section of the shell surface.

5. LINEAR VIBRATION ANALYSIS

A modal vibration can be written in the form

$$\tilde{u}(\eta,\theta,\tau)=\tilde{U}(\eta,\theta)\varphi(\tau) \qquad \tilde{v}(\eta,\theta,\tau)=\tilde{V}(\eta,\theta)\varphi(\tau) \qquad \tilde{w}(\eta,\theta,\tau)=\tilde{W}(\eta,\theta)\varphi(\tau) \tag{3}$$

where $\tilde{U}(\eta,\theta)$, $\tilde{V}(\eta,\theta)$, $\tilde{W}(\eta,\theta)$ is the linear mode shape previously obtained and $\varphi(\tau)$ is the nondimensional time law.

The mode shape is expanded by means of a double mixed series in terms of Chebyshev polynomials $T_m^*(\eta)$ in the axial direction and harmonic functions (cos $n\theta$, sin $n\theta$) in the circumferential direction

$$\tilde{U}(\eta,\theta)=\sum_{m=0}^{M_u}\sum_{n=0}^{N}\tilde{U}_{m,n}T_m^*(\eta)\cos n\theta \tag{4}$$

$$\tilde{V}(\eta,\theta)=\sum_{m=0}^{M_v}\sum_{n=0}^{N}\tilde{V}_{m,n}T_m^*(\eta)\sin n\theta \tag{5}$$

$$\tilde{W}(\eta,\theta)=\sum_{m=0}^{M_w}\sum_{n=0}^{N}\tilde{W}_{m,n}T_m^*(\eta)\cos n\theta \tag{6}$$

where $T_m^* = T_m(2\eta - 1)$, m denotes the Chebyshev polynomials order and n is the number of nodal diameters.

6. BOUNDARY CONDITIONS

Free-free boundary conditions are given by

$$\tilde{N}_x=0 \qquad \tilde{N}_{x\theta}+\tilde{M}_{x\theta}=0 \qquad \tilde{Q}_x+\frac{\partial\tilde{M}_{x\theta}}{\partial\theta}=0 \qquad \tilde{M}_x=0 \qquad \eta=0,1 \tag{7}$$

where the nondimensional force $(\tilde{N}_x,\tilde{N}_{x\theta},\tilde{Q}_x)$ and moment $(\tilde{M}_x,\tilde{M}_{x\theta})$ resultants are

$$\begin{aligned} &\tilde{N}_x=\tilde{\varepsilon}_{x,0}+\nu\tilde{\varepsilon}_{\theta,0} \qquad && \tilde{N}_{x\theta}=\frac{(1-\nu)}{2}\tilde{\gamma}_{x\theta,0} \qquad && \tilde{M}_x=\frac{\beta^2}{12}(\tilde{k}_x+\nu\tilde{k}_\theta)\\ &\tilde{M}_{x\theta}=\frac{\beta^2}{12}\frac{(1-\nu)}{2}\tilde{k}_{x\theta} \qquad && \tilde{Q}_x=\frac{\beta^2}{12}\left[\tilde{k}_{x,x}+\nu\tilde{k}_{\theta,x}+\frac{(1-\nu)}{2}\tilde{k}_{x\theta,\theta}\right] \end{aligned} \tag{8}$$

7. RAYLEIGH RITZ METHOD

The maximum number of variables needed for describing a general vibration mode with n nodal diameters is obtained by the relation ($N_p = M_u + M_v + M_w + 3 - p$), where ($M_u = M_v = M_w$) denote the order of the Chebyshev orthogonal polynomials and p describes the number of equations for the boundary conditions to be respected.

For a multi-mode analysis with different values of nodal diameters n, the number of degrees of freedom of the system is computed by the relation ($N_{max} = N_p \times (N + 1)$), where N represents the maximum value of the nodal diameters n considered.

Equations (3) are inserted into the expressions of the potential energy $\tilde{U}$ (1) and kinetic energy $\tilde{T}$ (2) to compute the Rayleigh quotient $R(\tilde{q}) = \tilde{U}_{\max} / \tilde{T}^*$, where $\tilde{U}_{\max} = \max(\tilde{U})$ is the maximum of the potential energy in a modal vibration, $\tilde{T}^* = \tilde{T}_{\max} / \omega^2$, $\tilde{T}_{\max} = \max(\tilde{T})$ is the maximum of the kinetic energy during a modal vibration, ω is the circular frequency of the motion $\varphi(\tau) = \cos \omega\tau$ and $\tilde{q} = [..., \tilde{U}_{m,n}, \tilde{V}_{m,n}, \tilde{W}_{m,n}, ...]^T$ is the vector of the unknowns.

After imposing the stationarity to the Rayleigh quotient, the following eigenvalue problem is obtained

$$(-\omega^2 \tilde{\boldsymbol{M}} + \tilde{\boldsymbol{K}})\tilde{\boldsymbol{q}} = \boldsymbol{0} \tag{9}$$

which furnishes approximate natural frequencies and mode shapes.

The approximate mode shape of the *j*-th mode is given by equations (4-6), where the coefficients $(\tilde{U}_{m,n}, \tilde{V}_{m,n}, \tilde{W}_{m,m})$ are substituted with $(\tilde{U}^{(j)}_{m,n}, \tilde{V}^{(j)}_{m,n}, \tilde{W}^{(j)}_{m,m})$, as the components of the *j*-th eigenvector $\tilde{q}_j$ of the equation (9).

The vector function

$$\tilde{\boldsymbol{Q}}^{(j)}(\eta,\theta) = \left[\tilde{U}^{(j)}(\eta,\theta),\ \tilde{V}^{(j)}(\eta,\theta),\ \tilde{W}^{(j)}(\eta,\theta)\right]^T \tag{10}$$

is the approximation of the *j*-th eigenfunction vector of the original problem.

8. NONLINEAR VIBRATION ANALYSIS

The three displacement fields $\tilde{u}(\eta,\theta,\tau), \tilde{v}(\eta,\theta,\tau), \tilde{w}(\eta,\theta,\tau)$ are expanded by using both the linear mode shapes $\tilde{U}(\eta,\theta), \tilde{V}(\eta,\theta), \tilde{W}(\eta,\theta)$ previously obtained and the conjugate mode shapes $\tilde{U}_c(\eta,\theta), \tilde{V}_c(\eta,\theta), \tilde{W}_c(\eta,\theta)$ in the form

$$\begin{aligned}
\tilde{u}(\eta,\theta,\tau) &= \sum_{j=1}^{N_u}\sum_{n=1}^{N}\left[\tilde{U}^{(j,n)}(\eta,\theta)\varphi_{u,j,n}(\tau) + \tilde{U}_c^{(j,n)}(\eta,\theta)\varphi_{u,j,n,c}(\tau)\right] \\
\tilde{v}(\eta,\theta,\tau) &= \sum_{j=1}^{N_v}\sum_{n=1}^{N}\left[\tilde{V}^{(j,n)}(\eta,\theta)\varphi_{v,j,n}(\tau) + \tilde{V}_c^{(j,n)}(\eta,\theta)\varphi_{v,j,n,c}(\tau)\right] \\
\tilde{w}(\eta,\theta,\tau) &= \sum_{j=1}^{N_w}\sum_{n=1}^{N}\left[\tilde{W}^{(j,n)}(\eta,\theta)\varphi_{w,j,n}(\tau) + \tilde{W}_c^{(j,n)}(\eta,\theta)\varphi_{w,j,n,c}(\tau)\right]
\end{aligned} \tag{11}$$

The Lagrange equations of motion for free vibrations are expressed in the form

$$\frac{d}{d\tau}\left(\frac{\partial \tilde{L}}{\partial \dot{\tilde{q}}_i}\right) - \frac{\partial \tilde{L}}{\partial \tilde{q}_i} = 0 \qquad i \in [1, N_{\max}] \qquad (\tilde{L} = \tilde{T} - \tilde{U}) \tag{12}$$

Using the Lagrange equations (12), a set of nonlinear ordinary differential equations is then obtained; such system is then solved by using numerical methods.

Table 1. Effective and equivalent parameters of the Single-Walled Carbon Nanotube [5].

Effective thickness h_0 (nm)	0.10 ÷ 0.15
Equivalent thickness h (nm)	0.066
Effective Young's modulus E_0 (TPa)	1.0 ÷ 2.0
Equivalent Young's modulus E (TPa)	5.5
Effective Poisson's ratio ν_0	0.12 ÷ 0.28
Equivalent Poisson's ratio ν	0.19
Surface density of graphite σ (kg/m^2)	7.718×10^{-7}
Equivalent mass density ρ (kg/m^3)	11700

9. NUMERICAL RESULTS

In order to study the discrete carbon nanotube as a continuum elastic thin shell, equivalent parameters must be considered [5]. These parameters are reported in Table 1.

The present model is then validated with the molecular dynamics data available in the literature [3]; the results reported in Table 2 show that the present model is accurate.

In Figures 2 (a-f), three mode shapes of a free-free carbon nanotube are presented, such modes are considered for the development of the semi-analytic nonlinear model of the carbon nanotube in the re-expansion of Equation (11).

In Figures 3-5, energy distributions in linear and nonlinear field are shown. Different modes are studied. The carbon nanotube is unwrapped on a plane to allow the energy representation. The damping is not considered and the total energy is constant (integral of density over the surface).

The sequence of Figures 3 (a-d) shows the distribution of the energy density [Jm^{-2}] in linear field for the modes (0,2), (2,2) in a time range.

The analysis of the total energy distribution over the nanotube surface shows a periodicity along the circumferential direction. Moreover, the energy is distributed symmetrically with respect to the longitudinal direction because two symmetric modes (0,2) and (2,2) are combined.

Figures 4 (a-d) show the distribution of the energy density in nonlinear field for the combined modes (0,2) and (2,2) in a time range. By comparing the linear and nonlinear analyses (with the same modal initial conditions), the nonlinear distribution evolves in a more complex patter, where the total energy periodicity and symmetry are preserved along the circumferential and longitudinal direction, respectively.

Table 2. Natural frequencies of the radial breathing mode ($j = 0$, $n = 0$): comparisons between Sanders-Koiter theory (SKT) and Molecular Dynamics Simulations (MDS).

Natural frequency (THz)			Difference %
(r, s)	SKT - Present model	MDS - Ref. [3]	
(10, 0)	8.966	8.718	2.84
(6, 6)	8.636	8.348	3.45
(12, 0)	7.478	7.272	2.83
(7, 7)	7.399	7.166	3.25
(8, 8)	6.473	6.275	3.15
(14, 0)	6.414	6.235	2.87
(16, 0)	5.606	5.455	2.77
(10, 10)	5.184	5.026	3.14

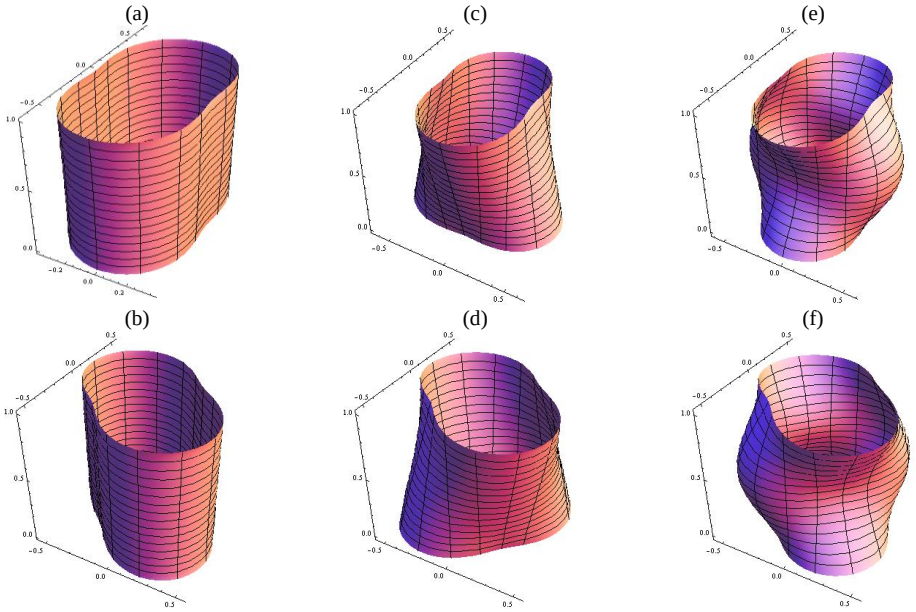

Figure 2. Mode shapes of the SWNT (r = 10, s = 0, L = 10 nm). Equivalent parameters. Free edges. Conjugate modes. (a),(b) Modes (0,2). (c),(d) Modes (1,2). (e),(f) Modes (2,2).

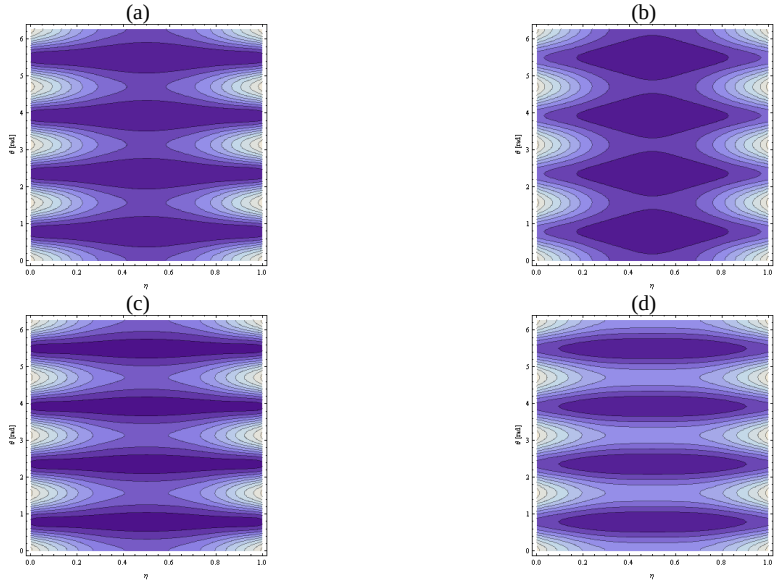

Figure 3. Total energy distribution $\tilde{E}$ (η, θ, τ). Combined modes (0,2), (2,2). Linear analysis. (a) τ = 0.00. (b) τ = 1.26. (c) τ = 2.51. (d) τ = 3.77.

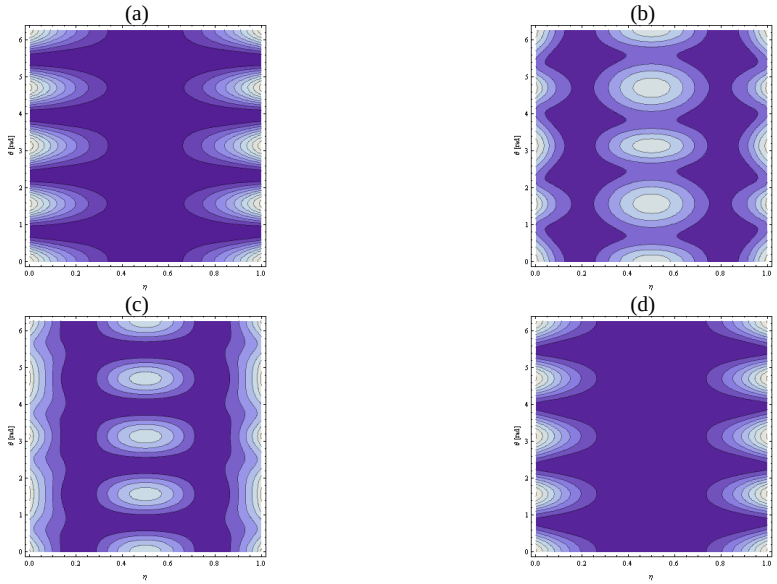

Figure 4. Total energy distribution $\tilde{E}(\eta, \theta, \tau)$. Combined modes (0,2), (2,2). Nonlinear analysis. (a) $\tau = 0.00$. (b) $\tau = 1.26$. (c) $\tau = 2.51$. (d) $\tau = 3.77$.

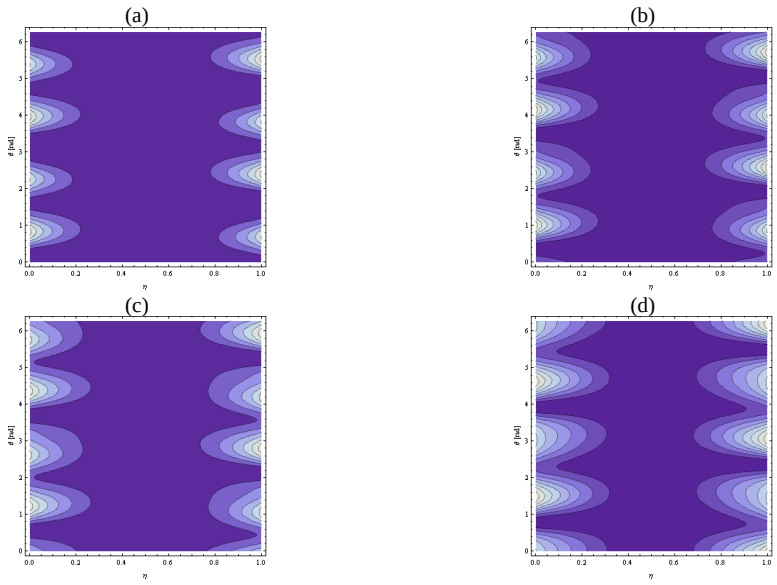

Figure 5. Total energy distribution $\tilde{E}(\eta, \theta, \tau)$. Conjugate modes (1,2). Nonlinear analysis. (a) $\tau = 8.00$. (b) $\tau = 8.02$. (c) $\tau = 8.04$. (d) $\tau = 8.06$.

The sequence of Figures 5 (a-d) shows the energy density distribution in nonlinear field for the two conjugate modes (1,2) in a time range. The periodicity along the circumferential direction is preserved.

The activation of the second mode implies an energy transfer between the conjugate modes. The participation of both the two conjugate modes gives rise to a travelling wave which moves circumferentially around the shell.

10. CONCLUSIONS

In this paper, the nonlinear vibrations of SWNTs are studied within the framework of the Sanders-Koiter elastic shell theory. The Rayleigh-Ritz method is applied in order to obtain approximate natural frequencies and mode shapes. The present model is validated in linear field with data available in the literature. An energy approach based on the Lagrange equations is considered to obtain a set of nonlinear ordinary differential equations. The total energy distribution is analysed in linear and nonlinear fields by assuming suitable initial conditions. The nonlinear energy distribution evolves in a complex pattern with periodicity along the circumferential direction. The participation of two conjugate modes gives rise to an energy transfer between the modes. The periodicity along the circumferential direction is preserved. A travelling wave moving circumferentially around the shell takes place.

REFERENCES

[1] Iijima S, 1991. "Helical microtubules of graphitic carbon", *Nature*, **354**, pp. 56-58.

[2] Rao AM, Richter E, Bandow S, Chase B, Eklund PC, Williams KA., Fang S, Subbaswamy K, Menon M, Thess A, Smalley RE, Dresselhaus G, and Dresselhaus MS, 1997. "Diameter-Selective Raman Scattering from Vibrational Modes in Carbon Nanotubes", *Science*, **275**, pp. 187-191.

[3] Gupta SS, Bosco FG, and Batra RC, 2011. "Wall thickness and elastic moduli of single-walled carbon nanotubes from frequencies of axial, torsional and inextensional modes of vibration", *Computational Materials Science*, **47**, pp. 1049-1059.

[4] Arghavan S, Singh AV, 2011. "On the Vibrations of Single-Walled Carbon Nanotubes", *Journal of Sound and Vibration*, **330**, pp. 3102-3122.

[5] Wang CY, Ru CQ, and Mioduchowski A, 2004. "Applicability and Limitations of Simplified Elastic Shell Equations for Carbon Nanotubes", *Journal of Applied Mechanics*, **71**, pp. 622-631.

[6] Strozzi M, Manevitch LI, Pellicano F, Smirnov VV, and Shepelev DS, 2014. "Low-frequency linear vibrations of Single-Walled Carbon Nanotubes: analytical and numerical models", *Journal of Sound and Vibration*, **333**, pp. 2936-2957.